



HAL
open science

Time-resolved Fluorescence and Generalized Polarization: Innovative tools to assess bull sperm membrane dynamics during slow freezing

Shaliha Bechoua, Pascale Winckler, Audrey Jossier, Caroline Peltier, Frédéric Delize, Noémie Devaux, Jean-Marie Perrier-Cornet, Hélène Simonin

► To cite this version:

Shaliha Bechoua, Pascale Winckler, Audrey Jossier, Caroline Peltier, Frédéric Delize, et al.. Time-resolved Fluorescence and Generalized Polarization: Innovative tools to assess bull sperm membrane dynamics during slow freezing. *Cryobiology*, 2019, 91, pp.69-76. 10.1016/j.cryobiol.2019.10.196 . hal-02354329

HAL Id: hal-02354329

<https://institut-agro-dijon.hal.science/hal-02354329>

Submitted on 21 Dec 2021

HAL is a multi-disciplinary open access archive for the deposit and dissemination of scientific research documents, whether they are published or not. The documents may come from teaching and research institutions in France or abroad, or from public or private research centers.

L'archive ouverte pluridisciplinaire **HAL**, est destinée au dépôt et à la diffusion de documents scientifiques de niveau recherche, publiés ou non, émanant des établissements d'enseignement et de recherche français ou étrangers, des laboratoires publics ou privés.



Distributed under a Creative Commons Attribution - NonCommercial 4.0 International License

35 **Abstract:**

36

37 During slow freezing, spermatozoa undergo membrane alterations that compromise their ability
38 of fertilizing. These alterations are caused either by cold shock or by the use of cryoprotectants
39 known to be cytotoxic. However, little is known about the membrane changes that occurred
40 during freezing. Here, we combined Generalized Polarization (GP), **Time-resolved**
41 **Fluorescence** and laurdan fluorescence properties to investigate the changes in membrane
42 fluidity and dynamics during slow freezing of bull sperm. We successfully demonstrated that
43 laurdan may be distributed in three different local environments that correspond to different
44 membrane lipid composition. These environments won't behave the same way when the cells
45 will be subjected to either a chemical treatment (adding the cryoprotectants) or a physical
46 treatment (freezing).

47

48

49

50

51

52

53

54

55

56

57

58

59

60

61

62

63

64

65

66

67

68

69 Introduction

70

71 Artificial insemination is a relevant technique in a dairy and meat cattle breeding
72 programme. Assisted reproduction and especially artificial insemination has played a central
73 role in livestock breeding. Hence, the success of artificial insemination requires
74 cryopreservation of semen for long periods of time.

75 Slow freezing of semen from genetically superior sires allows long storage and
76 distribution of doses of semen for insemination. Bull sperm cryopreservation techniques have
77 progressed slowly over the past several decades and the techniques are currently standardized.
78 The success of cryopreservation is based on adding cryoprotectants (for instance glycerol) to
79 extenders (diluent which is added to semen to preserve its fertilizing ability) and other
80 components such as egg yolk, milk, bovine serum albumin, polyvinyl alcohol and liposomes to
81 minimize the detrimental effects of freezing and thawing [7]. Cryoprotectants protect sperm
82 from cold shock, osmotic stress, membrane alterations (fluidity and permeability changes) plus
83 provide energy substrates for spermatozoa survival [7] [19].

84 Spermatozoa are known to be highly sensitive cells. These cells are highly polarized
85 and show extreme compartmentalization of its plasma membrane. Sperm cells are made of 3
86 domains : the head, a flagellum and a midpiece. The sperm head can be subdivided in 3 regions :
87 the acrosome, the equatorial segment and the postacrosome. Since sperm cells are
88 transcriptionally inactive and cannot synthesize any proteins, they have developed an
89 alternative strategy of sequestering proteins into different compartments until they are needed.
90 The process of sequential exposure of sperm proteins must be accurate to ensure successful
91 fertilization. The acrosome, the equatorial segment, and the postacrosome have distinct
92 subcellular structures and proteins. A study By Ellis et al. [13] using atomic force microscopy
93 (AFM) illustrated unique sperm surface topology of each domain that is distinguishable from
94 that of other domains [13] Maintaining the integrity of these domains after cryopreservation is
95 crucial for the fertilization process to occur.

96 Therefore, it is of great interest to get into the effect of slow freezing on sperm
97 functionality. It has been shown that approximately 50% of sperm are immotile when thawed
98 after cryopreservation and sperm that remain motile have their fertility capacity compromised
99 due to cryoinjury [34]. Furthermore, while vitrification is commonly used for oocytes

100 cryopreservation, slow freezing is still the only technique to be used in bull breeding program.
101 Indeed, vitrification requires the use of high concentrations of cryoprotectants and it is known
102 that various cryoprotectants have a negative impact on spermatozoa [29].

103 The process of freezing and thawing may cause irreversible damages to sperm [15].
104 Effects of cryopreservation on sperm function and the ability of spermatozoa to fertilize have
105 been studied extensively in many species, particularly in bull. Cryopreservation alters many
106 functions such as capacitation (induction of premature capacitation; cryo-capacitation),
107 acrosomal reaction (premature reaction), mitochondrial function and motility (reduced motility)
108 were the most significant alterations observed [10]. While most cryoprotectants are known to
109 show some toxicity to sperm [21], the exact mechanisms by which cryopreservation
110 (cryoprotectants and cold) affects sperm function are still not well understood.

111 Plasma membrane structure has been shown to have significant impact on spermatozoa
112 functionality and hence fertility [29]. Indeed, some membrane components such as cholesterol
113 plays a central role in maintaining the ability of spermatozoon to fertilize the oocyte. During
114 the cryopreservation process, efflux of cholesterol from sperm plasma membrane along with
115 influx of Na^+ and Ca^{2+} ions have been described to be major contributors to premature
116 capacitation (cryocapacitation) [10][11]. In addition, release of reactive oxygen species (ROS)
117 from dead or moribund spermatozoa present in the frozen semen doses, may alter membranes of
118 the remaining live sperm subpopulation [18] Therefore, maintaining the integrity of sperm cell
119 membrane components during the freezing-thawing process is essential to preserve
120 spermatozoa fertilization potential after thawing.

121 In the present work, we propose to study for the first time the impact of cryopreservation on
122 bull spermatozoa by advanced biophysical methods (Generalized Polarization and **Time-**
123 **resolved Fluorescence**) using the fluorophore laurdan. Laurdan is a lipophilic polarity-sensitive
124 dye that is widely used to study membrane dynamics [5]. Measuring lipid packing of
125 membranes with GP has been extensively done on cell models [28].

126 Mammalian sperm are strongly laterally organized cells. For example, membrane fluidity and
127 domain formation in the acrosomal and postacrosomal part of the mammalian sperm cell
128 membrane are key elements for membrane stabilization before capacitation and creation of
129 fusion competence after capacitation [30].

130 We believed that laurdan GP and **Time-resolved Fluorescence** could be used as sensitive tools
131 for evaluation of spermatozoa plasma membrane dynamics after freezing.

132 **Materials and Methods**

133

134 ***Animals, semen collection and semen processing***

135 Semen samples were obtained from Hostein bulls (n=6) who were clinically proven to be free
136 from any general or genital diseases. The bulls were housed at the Elva Novia agricultural
137 cooperative (Fontaines, France) and maintained under uniform feeding and housing conditions.
138 Ejaculates were collected using an artificial vagina. The semen samples were assessed for
139 volume, sperm concentration and percentage of motile spermatozoa.

140 Computer sperm motility analysis program (CASA, IVOS version, Hamilton thorne
141 Biosciences, MA, USA) was used to assess sperm motion characteristics. CASA was adjusted
142 for bovine semen analysis.

143 Ejaculates containing spermatozoa with > 80% forward motility and concentrations greater than
144 1.0×10^9 spermatozoa / ml were used in this study.

145

146 ***Sperm preparation for slow freezing and thawing***

147 After evaluation, semen was diluted with a commercial egg yolk extender (Optidyl® ; Biovet:
148 BP 62, 32500 Fleurance, France) (composition: Tris diluent, ionised egg yolk, glycerol,
149 antibiotics) in order to obtain a final concentration of semen of 15 to 20 million /per straw and
150 settle at RT for 10 minutes. Then, the extended semen was cooled slowly to 4°C over a
151 minimum of two hours. Subsequently semen was frozen at a programmed rate of -3°C / min
152 from +4 to -10 °C; -40°C / min from -10 to -100°C; -20°C / min from -100 to -140 °C in a
153 digital freezing machine (Digitcool, ...). Thereafter, the straws were plunged into liquid
154 nitrogen. After storage, the straws were thawed in a 37 °C water bath for 30 s immediately
155 before use. After thawing, spermatozoa motility percentage was assessed using a phase contrast
156 microscope with a warm slide and the sperm vitality was evaluated using the eosin-nigrosin
157 stain.

158

159 ***Laurdan Labeling of sperm cells***

160 Laurdan is a polarity probe; upon excitation, its emission undergoes a spectral shift due to the
161 reorientation of water molecules present in the glycerol backbone region of the membrane. This
162 shift can be correlated to the lipid phase [24]. In the gel phase, when no water is present, laurdan
163 emission peaks at 440 nm, whereas in the liquid crystalline phase the spectrum is red-shifted
164 ≈ 50 nm. This shift is quantified using the generalized polarization (GP) function. **Laurdan is a**
165 **fluorescent membrane probe sensitive to changes in the environment polarity (extent of water**

166 penetration into the bilayer surface). As the tighter packing of lipids in ordered compared to
167 disordered phases leads to less accessibility to water molecules, polarity is also an indicator of
168 lipid order. Polarity changes are shown by shifts in the Laurdan emission spectrum, which are
169 quantified by calculating the generalized polarization (GP): $GP = (I_{440} - I_{490}) / (I_{440} + I_{490})$
170 where I_{440} and I_{490} are the fluorescence emission intensities at 440 and 490 nm respectively.
171 Higher GP values are attributed to a more ordered lipid environment (sub-band at 440 nm),
172 lower GP values to a more disordered one (sub-band at 490 nm), with more membrane
173 hydration.

174 For the labeling experiments, fresh semen was diluted in TRIS buffer solution in order to obtain
175 the same final concentration than frozen/thawed sperm (10 to 20 times dilution, final
176 concentration 40-50 10^6 spermatozoa / ml). Spermatozoa were labeled with laurdan for 10 min
177 at 37 °C. Laurdan was dissolved to a concentration of 8mM in dimethylsulfoxide (DMSO) and
178 stored at - 20°C at the dark. In the laurdan-stained spermatozoa suspension, the amount of
179 DMSO was 0.02% (v/v) and a final concentration of laurdan of 1.6 μ M. After staining the
180 spermatozoa were centrifuged at 200g for 5 min, washed once and a swim-up was performed
181 as explained below.

182 The same procedure was applied to frozen/thawed spermatozoa. Briefly sperm was diluted in
183 TRIS buffer solution and labeling was performed as described above.

184

185 ***Incubation of fresh semen samples with Optidyl***

186 Experiments were performed in order to evaluate the effect of Optidyl® (Cryoprotectants
187 mixture) on GP and lifetimes values of fresh spermatozoa. To do so, spermatozoa before
188 labeling with laurdan were diluted and incubated for 10 min with Optidyl® (dilution factor 15:
189 same dilution factor than the one used when freezing bull sperm).

190 After incubation, the cells were washed once and resuspended in TRIS buffer and GP and
191 lifetimes were measured as described below.

192 GP and lifetimes were measured at both 37°C and 23°C. The cell suspensions that were
193 refrigerated from 37°C to 23°C were warmed from 23°C to 37°C.

194

195 ***Swim-up procedure***

196 After centrifugation (washing step), the supernatant was discarded and 4 ml of pre-warmed
197 TRIS buffer solution were gently layered on the top of the sperm pellet before the sample was
198 incubated at 37 °C for 30 min in the incubator. After incubation, 3.5 ml of supernatant was

199 aspirated into a 15 ml centrifuge tube to be used for spectroscopy and imaging. This technique
200 was performed in order to use only motile spermatozoa for the experiments.

201

202 ***Generalized Polarization using spectroscopy***

203 Polarity changes are detected by measuring shifts in the laurdan emission spectrum, and the
204 Generalized Polarization function (GP) was defined as a way of measuring this wavelength
205 displacement [28]. Laurdan GP is also presented as an accurate and sensitive indicator of lipid
206 order [2][5]. In the gel phase when no water is present, laurdan emission peaks at 440 nm
207 whereas in the liquid crystalline phase the spectrum shifts **of about** 50nm.

208 The steady state emission of laurdan was measured by a Fluorolog-3 spectrofluorometer
209 (HORIBA Jobin Yvon). For the temperature-dependent fluorescence intensity measurements,
210 the excitation wavelength was 370 nm. Fluorescence emission spectra were recorded between
211 400 and 600nm. The laurdan GP parameter was calculated using the following equation:

212

$$213 \text{ GP} = (I_{440} - I_{490}) / (I_{440} + I_{490})$$

214

215 where I_{440} and I_{490} are the fluorescence emission intensities at 440 and 490 nm respectively.

216 Experiments were conducted both at 37°C and 23°C.

217

218 ***Time-Resolved Fluorescence Spectroscopy***

219 The fluorescence lifetime is powerful to probe the molecular environment of a given
220 fluorophore. Fluorescence lifetime may be understood as the average amount of time that a
221 fluorophore remains in the excited state following excitation [16][3]. This parameter depends
222 of the environment and the **structure of the fluorophore**, but is independent of its
223 concentration. Each individual fluorescent molecule typically exists in a state with its own
224 characteristic lifetime. Due to the presence of multiple molecules with distinct lifetimes, the
225 overall fluorescence decay after an excitation pulse is inherently multiexponential. Each
226 component of the multiexponential decay reflects the fractional contribution of a specific form
227 of the fluorescent probe.

228 Laurdan fluorescence lifetime is sensitive to the hydration of the interface region [3] and
229 displays an **longer fluorescence lifetime** in less hydrated environments [21]. As the tighter
230 packing of lipids in ordered compared to disordered phases leads to less accessibility to water
231 molecules, laurdan lifetime is also an indicator of lipid order.

232

233 Laurdan Fluorescence lifetimes were measured using a time-correlated single-photon-counting
234 (TCSPC) system on a FluoroMax-4 spectrofluorometer (HORIBA Jobin Yvon). Fluorescence
235 lifetime decay curves were measured with a pulsed 370-nm diode. Detection was set to 465 nm
236 with a 6 nm bandpass. The lifetime was recorded on a 100 ns scale and measurements were
237 stopped when peak signal reached 10 000 counts. The Instrument Response Function (IRF) was
238 obtained using the diffusion of the excitation light on the sample at 370 nm.
239 DAS6 v6.1 software was used for TCSPC histogram analysis. As large deviation of chi-squared
240 values from unity ($\chi^2 > 1.5$) occurs when using mono or bi-exponential adjustments,
241 data fitting was established using a three-exponential decay equation. This provides three
242 fluorescent lifetimes with the corresponding fractional contributions.
243 For this experiment 3ml of a suspension of labeled spermatozoa were used. Experiments were
244 conducted both at 37°C and 23°C.

245

246 *Statistical analyses*

247 A Wilcoxon-Mann-Whitney test was computed with R 3.3.2 to test differences between fresh
248 and frozen spermatozoa samples on the different variables (GP and lifetimes). This test does
249 not require the assumption of normal distributions. P-values were calculated for each variable,
250 indicating significant differences when they are lower than 0.05.

251 The same tests were also computed to detect potential differences between 23⁰C and 37⁰C.

252 Sperm samples of six different bulls were collected. For each bull, one sample of fresh sperm
253 and one sample of frozen sperm were analyzed.

254

255

256

257

258

259

260

261

262

263

264

265

266

267 **Results**

268 ***Steady state spectra and GP of laurdan: fresh versus frozen/thawed bull sperm***

269 The effect of slow freezing and thawing on bull spermatozoa membrane was assessed using
270 laurdan emission spectral. Figure 1 shows representative laurdan emission spectra measured in
271 fresh and frozen-thawed samples at two different temperatures, 37°C and 23°C. Spectra from
272 the frozen-thawed sample show one band with the maximum emission centered at 430 nm with
273 no shift when temperature decreases from 37°C to 23°C. Spectra from fresh samples were
274 broader with a shoulder at 490 nm appearing at 37°C. The intensity of the shoulder decreases
275 when temperature decreases to 23°C, indicating a decreased polarity of the probe
276 microenvironment. The spectra of fresh samples were thus very different from the frozen-
277 thawed samples and display a higher intensity of the band centered at 490 nm. Furthermore, the
278 spectra of fresh samples evolve as the temperature decreases while spectra of frozen thawed
279 samples were stable with temperature decrease.

280

281 Laurdan GP was then calculated from the emission spectra. Indeed, laurdan GP can be used to
282 monitor the transition between the two phases gel and liquid-crystalline lipid of the plasma
283 membrane with good precision.

284 Our results indicate that at 37°C, GP values were significantly increased in frozen / thawed
285 spermatozoa compared to fresh spermatozoa (0.51 *versus* 0.30, $p= 0.004$). This was also the
286 case at 23°C (0.53 *versus* 0.4, $p= 0.044$) when comparing frozen / thawed spermatozoa to fresh
287 spermatozoa (See table 1).

288 When fresh spermatozoa were subjected to temperature variation (from 37°C to 23 °C), GP
289 value increased significantly (0.30 *versus* 0.40, $p= 0.04$). However, when frozen/thawed
290 spermatozoa were subjected to the same temperature variation, no significant variation of GP
291 was observed (0.51 *versus* 0.53, $p=0.33$) (See table 1).

292

293 ***Time-Resolved Fluorescence spectroscopy***

294 The results of the time-resolved fluorescence measurements with laurdan are shown in table 1.
295 The decay of fluorescence intensity was assumed to be tri-exponential function of 3 lifetimes
296 (T1, T2, T3). Temperature dependent (for T2) and state dependent (for T3) changes of lifetimes
297 were observed when comparing fresh *versus* frozen/thawed spermatozoa (Figures 2a and 2b).

298

299 T1 lifetime: no significant difference in terms of temperature and state (fresh versus
300 frozen/thawed)

301 For fresh and frozen/thawed spermatozoa, no significant variation of T1 lifetimes was observed
302 when spermatozoa were subjected to a variation of temperature or when fresh spermatozoa
303 were frozen (Table 1).

304

305 T2 lifetime : temperature dependent correlation of membrane order and dynamics

306 Whatever the state of spermatozoa concerned (fresh and frozen/thawed spermatozoa), a
307 significant increase of T2 lifetimes when spermatozoa were subjected to a variation of
308 temperature (from 37°C to 23°C) was observed (fresh spermatozoa: 3.7 ± 0.3 and 4.07 ± 0.2 at
309 37°C and 23°C respectively; $p=0.052$ and frozen / thawed: 3.6 ± 0.2 and 3.9 ± 0.1 at 37°C and
310 23°C respectively; $p=0.02$); see Table 1; Figure 2a

311 No significant differences were observed when comparing fresh versus frozen / thawed at either
312 37°C ($p=0.423$) and 23°C ($p=0.229$); see Table 1; Figure 2a.

313

314 T3 lifetime : treatment dependent correlation of membrane order and dynamics

315 A treatment dependent change (significant increase) of lifetimes were observed at 37°C and
316 23°C when comparing fresh versus frozen / thawed spermatozoa at 37 °C (9.2 ± 2.2 versus
317 12.5 ± 0.4 , $p=0.015$, % increase of 35.9%) and fresh versus frozen / thawed spermatozoa at 23
318 °C (8.9 ± 1.4 versus 12.8 ± 0.5 , $p=0.005$; % increase of 43.8%). See Table 1, Figure 2b.

319

320 **Weights of T1, T2 and T3: B1, B2 and B3**

321 The weights of T1, T2 and T3 were defined as B1, B2 and B3.

322

323 When comparing the weights of B1, B2 and B3 for fresh spermatozoa subjected to a variation
324 of temperature (37°C to 23°C), a significant difference was observed only for B3 (21.3% versus
325 31.6%; $p=0.04$), Table 1 and Figure 2c.

326 However, no significant variation was observed for frozen thawed spermatozoa subjected to a
327 variation of temperature (37°C to 23°C) whatever the proportion considered, Table 1 and
328 Figure 2c.

329

330 **Effect of Optidyl on fresh spermatozoa GP and lifetimes**

331 The effect of the cryoprotectant mixture Optidyl was measured on membrane dynamics so as
332 to differentiate the membrane modifications due to the cryoprotectants from the ones due to

333 freezing-thawing. For this purpose, spermatozoa were incubated with Optidyl and washed
334 before laurdan staining.

335

336 While incubation of spermatozoa with Optidyl had no effect on GP value measured at
337 37°C, it clearly impacted GP evolution during a temperature variation from 37 to 23°C and
338 subsequent warming to 37°C (37°C bis). Indeed, in fresh spermatozoa GP increases from 0.32
339 to 0.41 with decreasing temperature to 23 °C and decreases again to 0.30 when temperature get
340 back to 37°C. In fresh spermatozoa incubated with Optidyl, GP value remains stable at around
341 0.32 during the temperature variation. As already observed in [Table 1](#), frozen-thawed
342 spermatozoa had a significant higher GP value at 37°C (0.58) than fresh spermatozoa (0.32)
343 and fresh spermatozoa incubated with Optidyl (0.32); [Figure 3](#). Furthermore, their GP value
344 was stable (around 0.56) during the temperature variation as observed for fresh spermatozoa
345 incubated with Optidyl, see [Figure 3](#).

346

347 Regarding T2, the behavior was the same for the three types of spermatozoa, fresh, fresh
348 incubated with Optidyl and frozen-thawed. As already observed for the fresh and frozen-thawed
349 spermatozoa a significant increase of T2 was observed with temperature decrease to 23°C for
350 spermatozoa incubated with Optidyl (fresh without optidyl 37 °C: 3.52, *versus* Fresh without
351 optidyl 23 °C: 3.98) (fresh with optidyl at 37°C: 3.53 *versus* with optidyl at 23°C: 3.74).
352 Furthermore, the T2 variation was reversible with warming again to 37°C; see [Figure 4a](#).

353 The measurement of T3 gave interesting results as the T3 value increases for the fresh (9.83 at
354 37°C), incubated with Optidyl (12.14 at 37°C) and frozen-thawed spermatozoa (12.82 at 37°C)
355 respectively. T3 was independent of temperature variation for fresh spermatozoa and the ones
356 incubated with Optidyl; see [Figure 4b](#).

357

358

359

360

361

362

363

364

365

366

367 **Discussion**

368 Spermatozoa are very specific cells that are made of 5 regions known as the acrosome,
369 equatorial segment, postacrosome, midpiece and principal piece. They are polarized and
370 polarity is established during spermiogenesis in the testis. Spermatozoa plasma membrane
371 contains protein and lipids (free cholesterol and phospholipids represent 80% of sperm lipids).
372 Among the phospholipids, a high proportion of polyunsaturated fatty acids are susceptible to
373 oxidative stress (ROS: Reactive Oxygen Species).

374 Membrane lipids are correlated to specific functions, because they promote the creation of
375 microdomains with different fluidity and permeability characteristics required for the
376 fertilization process [33][30]. In addition, lipids are major determinant of motility, viability and
377 cell membrane integrity [27]. It has been shown in cat sperm, that cryopreservation significantly
378 impaired the plasma membrane integrity including the acrosome [32] that is why developing
379 techniques to study membrane integrity are of importance.

380 In the present work, we measured the fluorescence properties of laurdan in spermatozoa
381 membranes. Laurdan, a membrane dye [6], presents a large excited state dipole moment, which
382 results in its ability to report the extent of water penetration into the bilayer surface due to the
383 dipolar relaxation effect. Because water penetration has been correlated with lipid packing and
384 membrane fluidity [25], laurdan has been extensively used in membrane studies.

385 In our study, spermatozoa have undergone different treatments but are all motile because
386 selected by a swim-up procedure after staining. We thus assumed that the variations of
387 fluorescence properties of laurdan reflect modifications in the membrane lipids organization
388 and/or dynamics. Hence, spermatozoa, in which membrane traffic is virtually absent, offer a
389 good mammalian model in which laurdan properties can be exploited to study surface lipid
390 dynamics, since the absence of membrane traffic in sperm precludes label internalization [20].

391 Previous works demonstrated that a higher intensity of the band centered at 490 nm
392 indicates a higher polarity and a more fluid lipid phase [23]. Membranes of fresh sperm cells
393 respond to cooling to 23°C by a decrease of the emission spectra of laurdan at 490 nm resulting
394 in a higher GP value at 23°C than at 37°C. Thus, fresh sperm cells have functional membranes
395 able to respond to modifications of their environment by a decrease of fluidity.

396 Our results indicate that frozen-thawed spermatozoa display a decreased membrane
397 fluidity (higher GP value) in comparison to fresh spermatozoa at 37°C. Furthermore, the
398 emission spectrum of laurdan is not modified by a temperature decrease to 23°C. These results
399 indicate that membrane is altered by the freezing-thawing process.

400 Membrane fluidity is an important feature of spermatozoa fertility. An increased fluidity
401 of the sperm membrane has been shown to be associated with the acquisition of its fertilizing
402 ability [14]. Compositional and physicochemical alterations of bilayer features can greatly
403 affect the fertilizing ability of spermatozoa, for instance, modifying structural and functional
404 properties of proteins embedded in the bilayer [4]. Thus, modification of membrane fluidity
405 and behavior after freeze-thawing may lead to fertilization ability decrease of spermatozoa.

406
407 Interestingly, the cryoprotectant mixture Optidyl does not increase the GP values
408 however it prevents the increase of GP observed during a temperature change.
409 The extender used for semen dilution (Optidyl) maintains the biological environment necessary
410 for survival of spermatozoa and prevents membrane damages during cryopreservation. Egg
411 yolk (rich in phosphatidylcholine) in the semen extender is thought to regulate the efflux of
412 integral protein, phospholipids and cholesterol, and thus protects the plasma membrane against
413 temperature-related injury [14].

414 Studies conducted over the past two decades by Bergeron et al. [8] have revealed that a family
415 of lipid- binding proteins (BSP proteins) present in bull seminal plasma is detrimental to sperm
416 preservation as they induce cholesterol and phospholipid depletion from the plasma membrane.
417 Interestingly, low- density lipoproteins (LDL) present in egg yolk interact with the BSP
418 proteins, minimizing lipid removal from the sperm membrane. This phenomenon will
419 influence sperm storage in liquid or frozen states.

420
421 In the present work, we found that lifetime decay correlates well with a three exponential model,
422 meaning that laurdan molecules may be distributed in three different local environments. We
423 can argue that laurdan could be distributed in the three environments anterior acrosomal region,
424 posterior acrosomal region and equatorial segment, and that each environment corresponds to
425 a specific lifetime value. This difference in lifetimes values (T_1 : 0.7; T_2 : 3.7; T_3 : 9.2) is
426 presumably a reflection of the different lipid composition of the membranes in spermatozoa.

427 In particular, cholesterol in spermatozoa plays a crucial role in the biological processes that
428 occur during the fertilization process. Hence, the variation in cholesterol/phospholipids ratio
429 has been linked to the ability to survive cryopreservation [12].

430 It has been shown by freeze fracture [31] that cholesterol is densely packed in the anterior
431 acrosomal region as well as in the postacrosomal region while the equatorial region contains
432 very low level of cholesterol.

433

434 In addition, besides cholesterol, seminolipid is also of high importance in spermatozoa. Indeed,
435 seminolipid or SGG (SulfoGalactosylGlycerolipid) is present selectively and substantially in
436 mammalian germ cells. SGG consists of glycerol with a sn-1 alkyl and sn-2 acyl chain as the
437 lipid backbone, and a (3'sulfo)-galactopyranose β -linked to the sn-3 position. Throughout
438 mammalian species, C16:0/C16:0 (palmitoyl) SGG is the main molecular species.

439 In spermatozoa, it is an integral component of lipid rafts and it represents 10mol% of total
440 lipids. Since SGG is only present in sperm head, the % in this area accounts for more than
441 10mol%. SGG has been described to play a crucial role in mammalian male reproduction and
442 to be involved in sperm-zonal pellucida binding and sperm-egg plasma membrane binding [1].
443 The presence of SGG (which is known to be an ordered lipid) in sperm DRMs (detergent
444 resistant membranes) is due to its propensity to interact hydrophobically with cholesterol, a
445 pertinent component of DRMs [17]. Overall SGG would contribute to the biophysical
446 properties of the sperm head plasma membrane.

447 On none-reacted and none-capacitated sperm cells, SGG is present primarily at the apical ridge
448 subdomain of the plasma membrane of the spread head.

449 Hence, in terms of lipid composition, if we take not only into account cholesterol but also SGG,
450 the sperm head presents 3 lipid subdomains :

451 -anterior acrosomal region (apical ridge)

452 -equatorial segment

453 -posterior acrosomal region

454 The different lifetimes measured could thus be associated with the 3 head-regions.

455 T1, the shorter fluorescence lifetime, could be related to the presence of tightly packed lipid
456 domains, with less water accessibility. Due to their more dehydrated composition, the domains
457 associated to T1 are most probably less affected by the addition of cryoprotectants and freezing.

458

459 In our experiments, we observed that T3 does not vary with a variation of temperature. while
460 the freezing process affects T3 (increase of T3). The explanation to that, would be that in fresh
461 spermatozoa, cholesterol will stabilize the plasma membrane preventing any lifetime changes
462 during temperature changes and that the region that contains higher amount of cholesterol
463 would be associated to T3.

464 In addition, we observed that T3 irreversibly increased in frozen/thawed spermatozoa compared
465 to fresh spermatozoa. This could be explained by irreversible modification of lipid distribution
466 in membrane that took place during cryopreservation. This could be caused by the severe
467 osmotic stresses, sperm cells encounter during cryopreservation and thawing. This occurs with

468 addition and removal of cryoprotective agents, as well as during freezing and thawing [26].
469 Sperm are exposed to hypertonic conditions upon extracellular ice formation, because the solute
470 concentration in the extracellular unfrozen fraction increases. These results in cellular
471 dehydration due to water transport out of the cell to retain equilibrium between the intra- and
472 extracellular solute concentrations. Dehydration especially occurs when low cooling rates are
473 used for freezing. During thawing, the reverse process takes place, and sperm are exposed to
474 hypotonic conditions resulting in water uptake and swelling.

475 Such osmotic stress has been shown to be the predominant cause of cell damage [20].
476 Furthermore, T3 also increased with the Optidyl contact to spermatozoa. It can be hypothesized
477 that some components of Optidyl diffused into the plasma membrane. This would partly explain
478 the T3 increase.

479

480 Morris et al. (2007)[20] used cryo-scanning electron microscopy and freeze substitution to
481 show that no intracellular ice is formed in sperm. They claim that cell damage predominantly
482 results from an osmotic imbalance encountered during thawing. Hence, conducting to membrane
483 deshydration after freezing.

484

485 We have shown that laurdan fluorescence lifetime can be either treatment dependant (T3) or
486 temperature dependant (T2) and that optidyl along with the freezing process are going to
487 prevent the plasma membrane dynamics during a change of temperature (no variation of the
488 proportion of lifetimes). Our results indicate that plasma membrane environments associated to
489 each fluorescence lifetime value wont behave the same way when the cells will be subjected to
490 either a chemical treatment (adding the cryoprotectants) or a physical treatment (freezing). As
491 for T1

492

493

494 The clear-cut relationships between laurdan spectral properties and membrane structure
495 and dynamics makes laurdan spectroscopy a useful tool in investigating the correlations
496 between the physical properties of the membrane environment and sperm functions. Our work
497 demonstrated for the first time that Fluorescence Life Time Spectroscopy and Generalized
498 Polarization could be used as innovative tools to evaluate bull's plasma membrane dynamics
499 during the freezing process.

500

501

502 **Acknowledgments**

503 We would like to thank the cooperative Elva Novia (Fontaines, FRANCE) for providing us in
504 bull sperm and also the Regional Council of Bourgogne – Franche Comté and the “Fonds
505 Européen de DEveloppement Régional (FEDER) for funding this project.

506

507 **Competiting interests**

508 The author(s) declare(s) that there is no conflict of interest regarding the publication of this
509 article.

510

511 **Funding**

512 This work was supported by the Regional Council of Bourgogne – Franche Comté, the
513 “Fonds Européen de DEveloppement Régional (FEDER)”

514

515

516

517

518

519

520

521

522

523

524

525

526

527

528

529

530

531

532

533

534

535 **References**

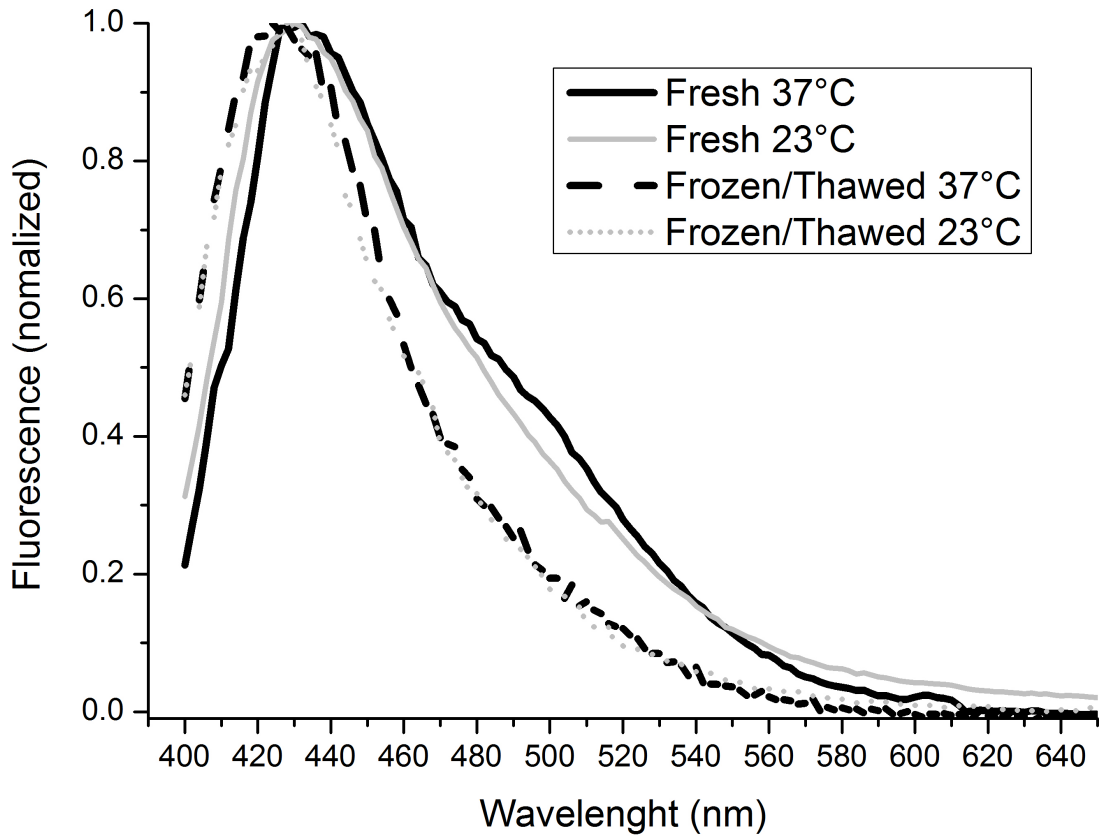
- 536 [1] V. Ahnonkitpanit et al., « Role of egg sulfolipidimmobilizing protein 1 on mouse sperm-
537 egg plasma membrane binding », *Biol. Reprod.*, 61 (1999) 749-756
538
- 539 [2] M. Amaro, R. Šachl, P. Jurkiewicz, A. Coutinho, M. Prieto, et M. Hof, « Time-Resolved
540 Fluorescence in Lipid Bilayers: Selected Applications and Advantages over Steady
541 State », *Biophys. J.*, 107 (2014) 2751-2760
542
- 543 [3] M. Amaro, F. Reina, M. Hof, C. Eggeling, et E. Sezgin, « Laurdan and Di-4-ANEPPDHQ
544 probe different properties of the membrane », *J. Phys. Appl. Phys.*, 50 (2017), 134004
545
- 546 [4] A. Ambrosini, G. Zolese, G. Balercia, E. Bertoli, G. Arnaldi, et F. Mantero, « Laurdan
547 fluorescence: a simple method to evaluate sperm plasma membrane alterations », *Fertil.*
548 *Steril.*, 76 (2001) 501-505
549
- 550 [5] L. A. Bagatolli, T. Parasassi, G. D. Fidelio, et E. Gratton, « A model for the interaction of
551 6-lauroyl-2-(N,N-dimethylamino)naphthalene with lipid environments: implications for
552 spectral properties », *Photochem. Photobiol.*, 70 (1999) 557-564
553
- 554 [6] L. A. Bagatolli, « Monitoring Membrane Hydration with 2-(Dimethylamino)-6-
555 Acynaphtalenes Fluorescent Probes », *Subcell. Biochem.*, 71 (2015), 105-125
556
- 557 [7] F. Batellier *et al.*, « Advances in cooled semen technology », *Anim. Reprod. Sci.*, 68 (2001)
558 181-190
559
- 560 [8] A. Bergeron et P. Manjunath, « New insights towards understanding the mechanisms of
561 sperm protection by egg yolk and milk », *Mol. Reprod. Dev.*, 73 (2006). 1338-1344
562
- 563 [9] S. Büyükleblebici *et al.*, « Cryopreservation of bull sperm: Effects of extender
564 supplemented with different cryoprotectants and antioxidants on sperm motility,
565 antioxidant capacity and fertility results », *Anim. Reprod. Sci.*, 150 (2014) 77-83
566
- 567 [10] N. Cormier, M. A. Sirard, et J. L. Bailey, « Premature capacitation of bovine spermatozoa
568 is initiated by cryopreservation », *J. Androl.*, 18 (1997) 461-468
569
- 570 [11] N. Cormier et J. L. Bailey, « A differential mechanism is involved during heparin- and
571 cryopreservation-induced capacitation of bovine spermatozoa », *Biol. Reprod.*, 69 (2003)
572 177-185
573
- 574 [12] A. Darin-Bennett et I. G. White, « Influence of the cholesterol content of mammalian
575 spermatozoa on susceptibility to cold-shock », *Cryobiology*, vol. 14 (1977) 466-470,
576
- 577 [13] D. J. Ellis et al., « Post-testicular development of a novel membrane substructure within
578 the equatorial segment of ram, bull, boar, and goat spermatozoa as viewed by atomic force
579 microscopy », *Journal of Structural Biology*, 138 (2002) 187-198
580
- 581 [14] M. Forouzanfar *et al.*, « In vitro comparison of egg yolk-based and soybean lecithin-based

- 582 extenders for cryopreservation of ram semen », *Theriogenology*, 73 (2010), 480-487
583
- 584 [15] H. M. Harshan, L. P. Singh, A. Arangasamy, M. R. Ansari, et S. Kumar, « Effect of buffalo
585 seminal plasma heparin binding protein (HBP) on freezability and in vitro fertility of
586 buffalo cauda spermatozoa », *Anim. Reprod. Sci.*, 93 (2006) 124-133
587
- 588 [16] H. C. Ishikawa-Ankerhold, R. Ankerhold, et G. P. C. Drummen, « Advanced fluorescence
589 microscopy techniques--FRAP, FLIP, FLAP, FRET and FLIM », *Mol. Basel Switz.*, 17
590 (2012) 4047-4132
591
- 592 [17] M. B. Khalil *et al.*, « Sperm capacitation induces an increase in lipid rafts having zona
593 pellucida binding ability and containing sulfogalactosylglycerolipid », *Developmental
594 Biology*, vol. 290, n° 1, p. 220-235, févr. 2006.
595
- 596 [18] E. de Lamirande, C. Tsai, A. Harakat, et C. Gagnon, « Involvement of reactive oxygen
597 species in human sperm arcsome reaction induced by A23187, lysophosphatidylcholine,
598 and biological fluid ultrafiltrates », *J. Androl.*, 19 (1998) 585-594
599
- 600 [19] C. M. O. Medeiros, F. Forell, A. T. D. Oliveira, et J. L. Rodrigues, « Current status of
601 sperm cryopreservation: why isn't it better? », *Theriogenology*, 57 (2002) 327-344.,
602
- 603 [20] G. J. Morris, K. Faszer, J. E. Green, D. Draper, B. W. W. Grout, et F. Fonseca, « Rapidly
604 cooled horse spermatozoa: loss of viability is due to osmotic imbalance during thawing,
605 not intracellular ice formation », *Theriogenology*, 68 (2007) 804-812
606
- 607 [21] L. Olexikova, M. Miranda, B. Kulikova, A. Baláži, et P. Chrenek, « Cryodamage of
608 plasma membrane and acrosome region in chicken sperm », *Anat. Histol. Embryol.*, vol.
609 48 (2019) 33-39
610
- 611 [22] D. M. Owen, A. Magenau, D. Williamson, et K. Gaus, « The lipid raft hypothesis revisited
612 – New insights on raft composition and function from super-resolution fluorescence
613 microscopy », *BioEssays*, 34 (2012) 739-747
614
- 615 [23] S. Palleschi et L. Silvestroni, « Laurdan fluorescence spectroscopy reveals a single liquid-
616 crystalline lipid phase and lack of thermotropic phase transitions in the plasma membrane
617 of living human sperm », *Biochim. Biophys. Acta BBA - Biomembr.*, vol. 1279 (1996)
618 197-202
619
- 620 [24] T. Parasassi, E. K. Krasnowska, L. Bagatolli, et E. Gratton, « Laurdan and Prodan as
621 Polarity-Sensitive Fluorescent Membrane Probes », *J. Fluoresc.*, 8 (1998) 365-373
622
- 623 [25] T. Parasassi et E. Gratton, « Membrane lipid domains and dynamics as detected by
624 Laurdan fluorescence », *J. Fluoresc.*, 5 (1995) 59-69
625
- 626 [26] D. E. Pegg, « Principles of cryopreservation », *Methods Mol. Biol. Clifton NJ*, vol. 1257
627 (2015) 3-19
628
- 629 [27] J. A. Rooke, C. C. Shao, et B. K. Speake, « Effects of feeding tuna oil on the lipid
630 composition of pig spermatozoa and in vitro characteristics of semen », *Reprod. Camb.*

631 *Engl.*, 12 (2001) 315-322
632
633 [28] S. A. Sanchez, M. A. Tricerri, et E. Gratton, « Laurdan generalized polarization
634 fluctuations measures membrane packing micro-heterogeneity in vivo », *Proc. Natl. Acad.*
635 *Sci. U. S. A.*, 109 (2012) 7314-7319
636
637 [29] H. Sieme, H. Oldenhof, et W. Wolkers, « Sperm Membrane Behaviour during Cooling
638 and Cryopreservation », *Reprod. Domest. Anim.*, 50 (2015) 20-26
639
640 [30] C. D. Stubbs et A. D. Smith, « The modification of mammalian membrane polyunsaturated
641 fatty acid composition in relation to membrane fluidity and function », *Biochim. Biophys.*
642 *Acta*, 779 (1984) 89-137
643
644 [31] J. Tesařík et J.-E. Fléchon, « Distribution of sterols and anionic lipids in human sperm
645 plasma membrane: Effects of in vitro capacitation », *J. Ultrastruct. Mol. Struct. Res.*, 97
646 (1986) 227-237
647
648 [32] A. I. S. B. Villaverde *et al.*, « Cryoprotective effect of different glycerol concentrations
649 on domestic cat spermatozoa », *Theriogenology*, 80(2013) 730-737
650
651 [33] S. R. Wassall et W. Stillwell, « Polyunsaturated fatty acid-cholesterol interactions: domain
652 formation in membranes », *Biochim. Biophys. Acta*, 1788 (2009) 24-32
653
654 [34] P. F. Watson, « The causes of reduced fertility with cryopreserved semen », *Anim. Reprod.*
655 *Sci.*, vol. 60-61, n° Supplement C, (2000) 481-492
656
657
658
659
660
661
662
663
664
665
666
667
668
669
670
671
672

673

674 Figure 1 : Representative normalized steady-state emission spectra of Laurdan labelled fresh
675 sperm cells and frozen/thawed sperm cells. GP measurements were conducted both at 37°C
676 and 23 °C
677



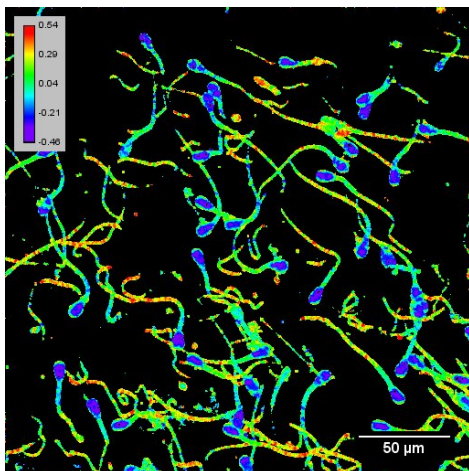
678

679 GP images of spermatozoa labelled with Laurdan using a false color scale

680

681

682



683

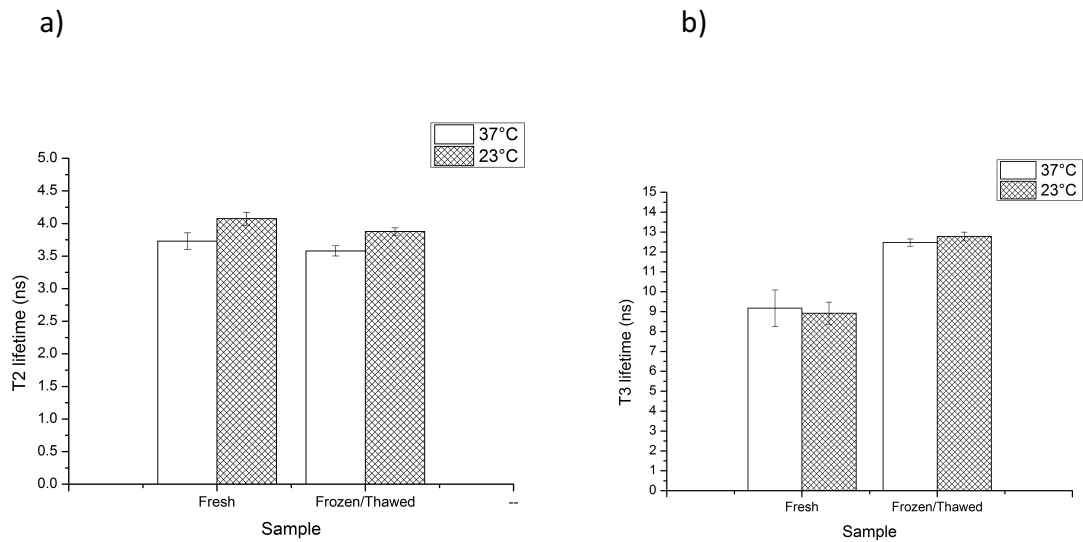
684

685

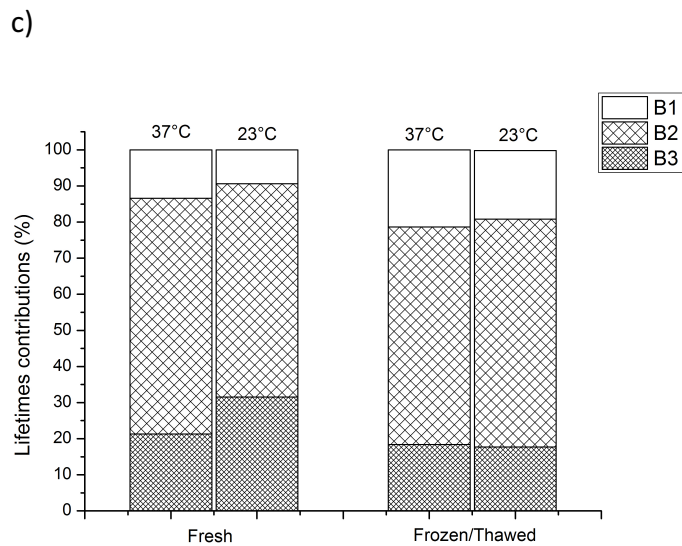
686 **Figure 2 : Time-Resolved Fluorescence Spectroscopy (T2 and T3) in fresh and frozen:thawed**
687 **spermatozoa at 23⁰C and 37⁰C (2a and 2b)**

688 **Weights B1, B2 and B3 of T1, T2 and T3 respectively in fresh and frozen/thawed spermatozoa**
689 **at 37⁰C and 23⁰C, 2c**

690
691
692
693
694
695

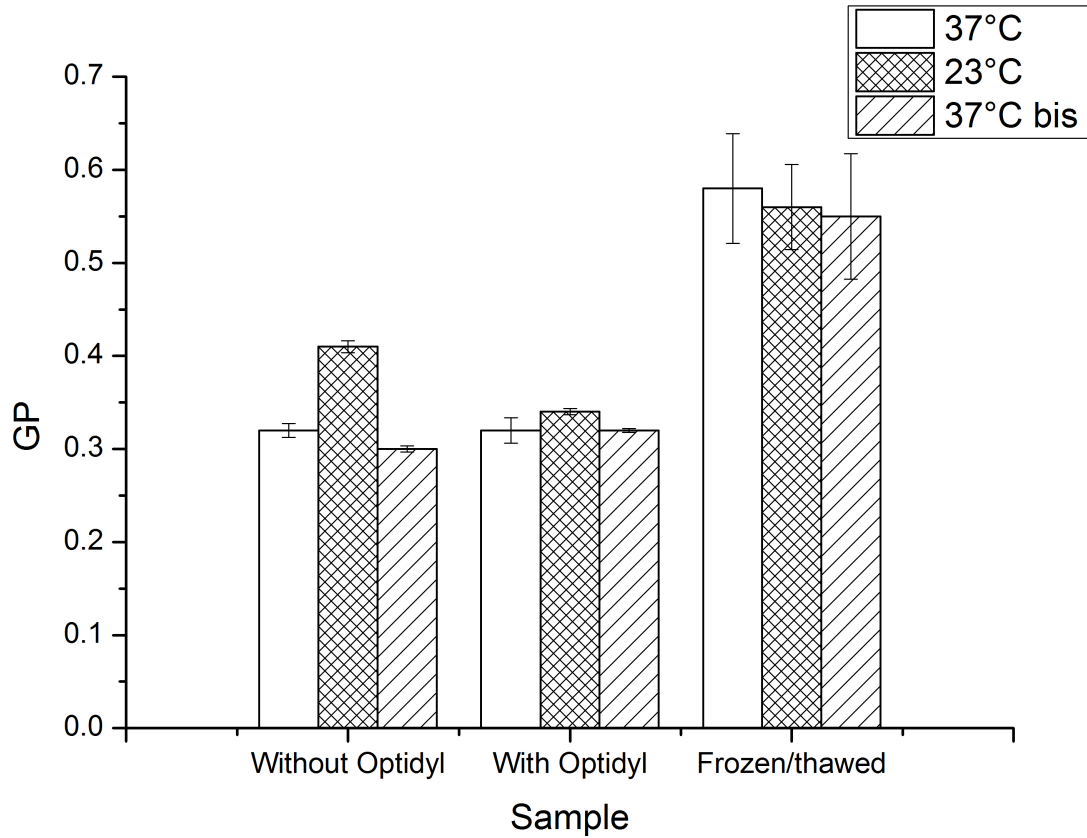


696
697
698
699
700
701
702
703



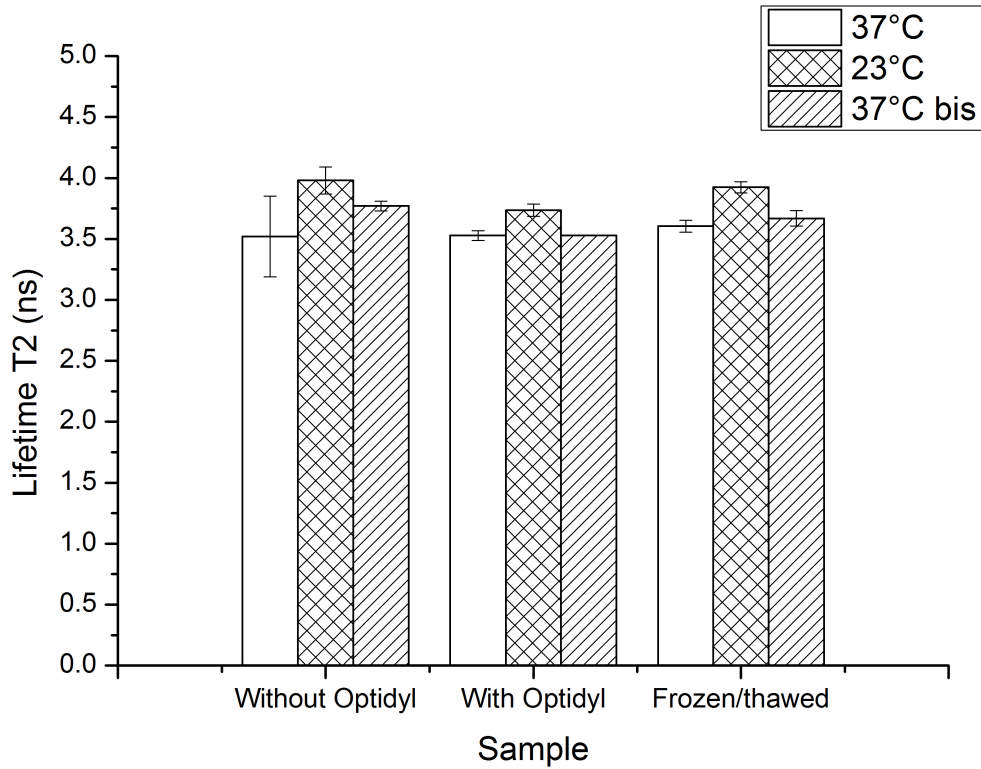
704
705
706
707
708
709
710

711 **Figure 3** : Effect of Optidyl on GP. GP was measured on spermatozoa incubated first at 37°C,
712 then at 23°C and again at 37°C. (37°C bis). For comparison, results obtained on frozen/thawed
713 spermatozoa were presented.
714
715

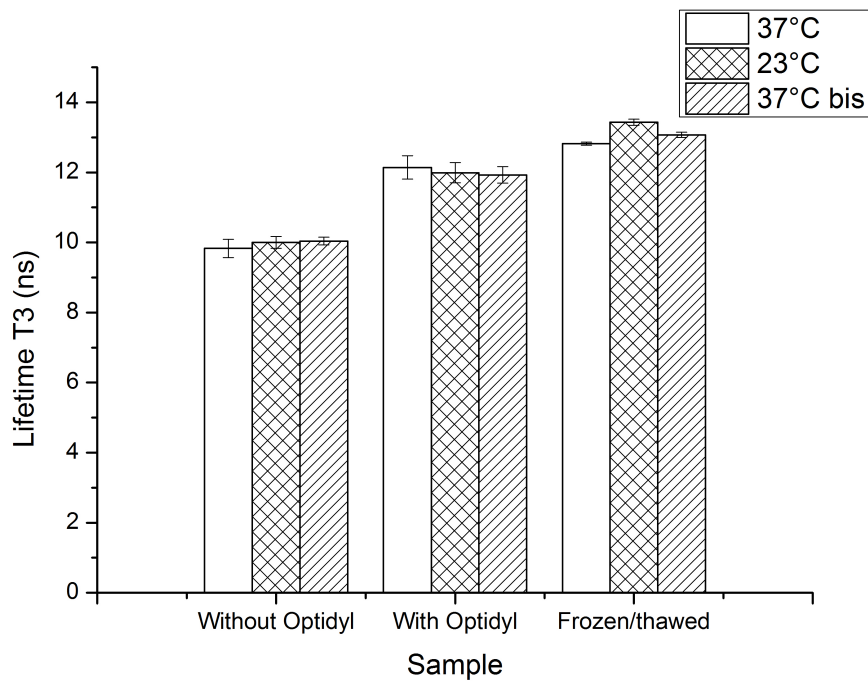


716
717
718
719
720
721
722
723
724
725
726
727
728
729
730
731
732
733
734
735
736

737 **Figure 4** : Effect of Optidyl on lifetimes (T2 and T3) and B weights on fresh spermatozoa. T and
 738 B were measured on spermatozoa incubated first at 37°C, then at 23°C and again at 37°C.
 739 (37°C bis). For comparison, results obtained on frozen/thawed spermatozoa were presented.
 740
 741 a)

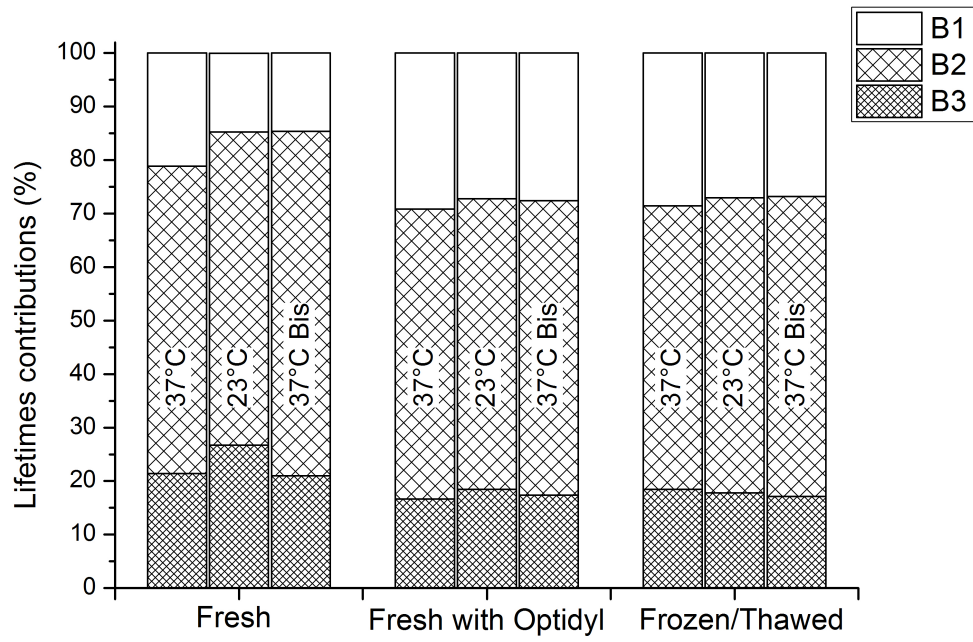


742
 743 b)



744
 745
 746
 747

748 c)



749
750
751
752
753
754
755
756
757
758
759
760
761
762
763
764
765
766
767
768
769
770
771

772 Table 1: table presenting T values ± SD in fresh versus frozen/thawed spermatozoa at 37⁰C and 23⁰C

773

774

	Fresh				Frozen/Thawed				P-values fresh vs Frozen/Thawed		P-values 37°C vs 23°C	
	37°C		23°C		37°C		23°C		37°C	23°C	Fresh	Frozen/Thawed
	Mean	Standard deviation	Mean	Standard deviation	Mean	Standard deviation	Mean	Standard deviation				
T1 (ns)	0,7	0,3	0,8	0,3	0,6	0,2	0,7	0,2	0,748	0,470	0,589	0,377
T2 (ns)	3.7*	0,3	4.07*	0,2	3.6**	0,2	3.9**	0,1	0,423	0,229	0,052	0,020
T3 (ns)	9,2	2,2	8,9	1,4	12,5	0,4	12,8	0,5	0,015	0,005	0,937	0,470
B1 (%)	13,4	8,4	9,4	4,5	21,3	6,1	19,0	6,8	0,093	0,030	0,485	0,470
B2 (%)	65,3	8,7	59,0	7,3	60,3	7,4	63,3	7,8	0,310	0,485	0,240	0,485
B3 (%)	21.3*	7,7	31.6*	9,8	18,4	2,3	17,7	2,3	0,173	0,002	0,041	0,688
GP	0.3*	0,02	0.4*	0,03	0.51*	0,09	0,53	0,08	0,005	0,045	0,005	0,334

776